

University of Arkansas, Fayetteville

ScholarWorks@UARK

Anthropology Undergraduate Honors Theses

Anthropology

5-2023

The Scaling Method: Body Mass Reconstruction of East African Hominins

Julianna Rose

Follow this and additional works at: <https://scholarworks.uark.edu/anthuht>



Part of the [Biological and Physical Anthropology Commons](#), and the [Evolution Commons](#)

Citation

Rose, J. (2023). The Scaling Method: Body Mass Reconstruction of East African Hominins. *Anthropology Undergraduate Honors Theses* Retrieved from <https://scholarworks.uark.edu/anthuht/9>

This Thesis is brought to you for free and open access by the Anthropology at ScholarWorks@UARK. It has been accepted for inclusion in Anthropology Undergraduate Honors Theses by an authorized administrator of ScholarWorks@UARK. For more information, please contact scholar@uark.edu.

The Scaling Method: Body Mass Reconstruction of East African Hominins

An Honors Thesis submitted in partial fulfillment of the requirements for Honors Studies in
Anthropology

By

Julianna Rose

Spring 2023

Anthropology

Fulbright College of Arts and Sciences

The University of Arkansas

Acknowledgements

I am extremely grateful to Dr. Plavcan for advising me throughout the research and writing process for this thesis. Additionally, I would like to thank the National Museums of Kenya for providing access to the digital 3-D fossil models that were studied in this project. I also acknowledge the members of my committee for their time and effort to evaluate my work. And finally, I would like to thank the faculty and staff of the Honors College for their guidance.

Table of Contents

Introduction	1
Methods	3
Results	7
Analysis	14
Discussion	16
Conclusion	18
List of References	20

Introduction

Body mass is an area of interest in the study of living and nonliving organisms, as it reflects how they interact with their environment. It is particularly useful for the analysis of extinct species because it indicates behaviors, diet, and lifestyle patterns that cannot be observed in the same manner as living species (Anton et al. 2014, Uhl et al. 2013, Grabowski et al. 2015, Will et al. 2017). Knowing the body size of fossils is especially useful because it implies how behaviors, lifestyle, and environmental interaction changed as species evolved. Within hominins, it is known that early *Homo* species were larger than their ancestors as a result of their dietary habits and adaptations for bipedality and migration (Anton et al. 2014, Grabowski et al. 2015). As depicted in the fossil record, *Australopithecus* and *Paranthropus* were consistently smaller than *Homo*, and early *Homo* was smaller than *Homo erectus* and modern humans (Anton et al. 2014, Grabowski et al. 2015, Will et al. 2017). These changes in body mass as new species emerged indicate an improvement in dietary quality and nutritional sufficiency as well as a predisposition for lower mortality (Anton et al. 2014).

A considerable portion of hominin body mass estimates draw upon the size and shape of the femur. Femora are frequently preserved in the fossil record, and they are of particular interest in the study of hominins because they present key information about the evolution of bipedal locomotory patterns (Grabowski et al. 2015). In addition to generally being larger than members of earlier hominin genera, *Homo* femora show significant anatomical variation in the minimum mediolateral breadth and have relatively straight shafts (Churchill and Vansickle 2007). Additionally, *Homo* femora have a larger head breadth, shorter neck, and greater lateral flare of the greater trochanter (Holliday et al. 2010). There is substantial morphological overlap between *Australopithecus* and early *Homo*, but early *Homo* are thought to have been larger on average

than *Australopithecus* (Anton et al. 2014). The anatomical features of the femur are exceptionally important for inferring locomotory patterns and lifestyle from the fossil record, but because of its role in weight bearing, the size of the femur is also tightly correlated with body mass, making it an attractive option for body mass estimation studies.

Many biological anthropologists have attempted to estimate early hominin body masses from fossil femora through various comparative methods. These can be separated into the broad categories of mechanical and morphometric methods, where mechanical methods seek to reconstruct body mass through analysis of weight bearing skeletal elements such as femoral head breadth, and morphometric methods attempt to estimate body mass based on the direct assessment of size and shape through measurements such as stature (Auerbach and Ruff 2004). Mechanical and morphometric approaches are equally reliable for estimating body mass, so the decision of which one to use depends on which structures are present in the fossil of interest. Throughout the past few decades, several body mass equations have been derived through these techniques, most commonly using an inverse calibration approach with a regression equation that represents body mass as a function of a particular skeletal measurement such as femoral head breadth or stature (Ruff 1991, McHenry 1992, Ruff 1994, Grine et al. 1995, Kappelman 1996, Ruff et al. 1997, Auerbach and Ruff 2004, Spocter and Manger 2007, Uhl et al. 2013, Grabowski et al. 2015, Elliot et al. 2016, Niskanen et al. 2018).

This project utilizes the most recently derived regression equations (Niskanen et al. 2018) to estimate body mass based on the femoral head breadth, which was obtained through three different techniques. The conventional approach in these studies is to directly measure the diameter of the femoral head, but that is often limited due to the fragmentary nature of fossils. Some studies suggest alternative methods that attempt to reconstruct the full head in order to get

the most accurate breadth measurement. One such technique is the sphere-fitting approach, which has been used in the past to support acetabulum measurements for body mass reconstruction (Hammond et al. 2013, Plavcan et al. 2014). The sphere-fitting method attempts to approximate the size of the femoral head and acetabulum through the creation of a 3-D sphere primitive in computer modeling software. This is particularly useful in cases where less than half of the head is present in the fossil because it relies upon the curvature of the fragment that exists, eliminating the need for a full cross-sectional diameter measurement. A similar but less common approach is using point cloud registration in 3-D modeling software. While this method predominantly measures the degree of variation in the shape of two models, it can also be used to evaluate the exact size difference between them (Mahfouz et al. 2007).

For this study, body masses were estimated from fossil femoral head breadths using a combination of direct measurement, sphere-fitting, and alignment techniques. The overall goal was to investigate whether the point cloud registration approach produces body mass results that are equivalent to the direct measurement and sphere-fitting approaches, which have demonstrated their reliability in prior studies. If the alignment method produces accurate results for body mass, it can serve as another tool for scientists to use when estimating body mass from fragmentary fossils.

Methods

This study drew upon a collection of East African fossils that were laser scanned and subsequently prepared by JM Plavcan, removing all bits of matrix and damaged surfaces. They were developed into 3-D models that could be analyzed entirely using computer software. Among the collection, the five fossils that contained at least a partial femoral head were included. All model calculations, measurements, and analyses were conducted in Cloud

Compare, a point cloud 3-D modeling software. This program was selected because it allowed efficient manipulation of the models in a digital 3-D space, and it could perform precise alignment and point cloud registration. The first step in the analysis of the sample was to take measurements using the point picking tool. The maximum diameter of the femur was approximated by selecting two points and computing the distance between them. The first point was placed at the fovea of the femur and the second was placed approximately where the neck began, as depicted in Figure 1. This process was repeated five times on separate days, and an average of the measurements was taken.

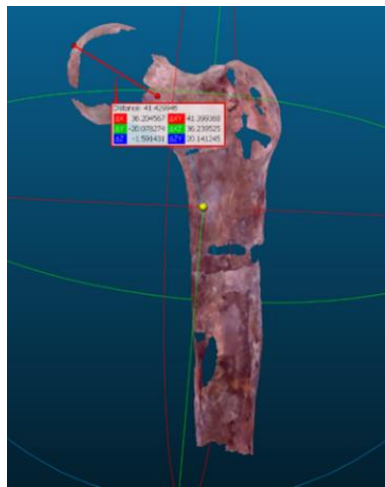


Figure 1: Direct Measurement of the Femoral Head Diameter

This image represents the measurement of the femoral head breadth (SI diameter) starting at the fovea and ending at the beginning of the neck, with the goal of measuring the longest segment.

The next step in analysis of the models was to create a sphere primitive that would approximate the diameter of the femoral head, eliminating the guesswork in estimating the longest segment of the head. This was performed using the “primitive factory” in the software, where an initial sphere with a 15 mm radius was generated and aligned with the femoral head of the fossil. The radius was then gradually increased until the sphere appeared larger than the head,

as shown in Figure 2. Like the direct measurements, this process was repeated five times on separate days, and an average of the values was taken.

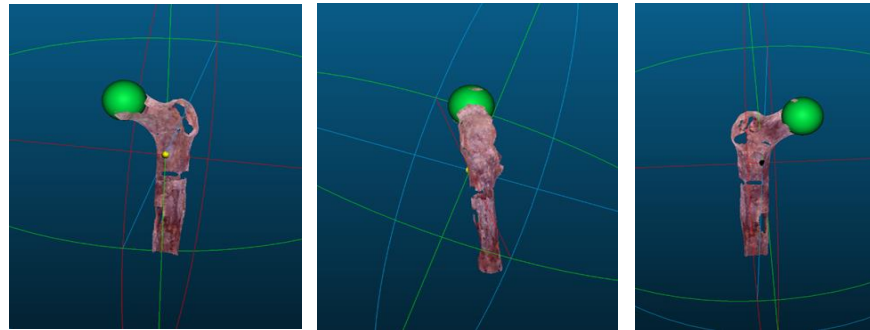


Figure 2: Sphere Approximation of the Femoral Head

Proceeding from left to right, these images demonstrate an anterior, lateral, and posterior view of a fossil femur with a sphere primitive approximating its femoral head breadth. The curvatures of the sphere are lined up with the curvatures present in the fossil, and it is scaled to best fit the size of the fossil's femoral head.

The next step was to align the fossils with human references to test the accuracy of the alignment approach. Before performing alignment and registration, a sample of modern human femur models were selected to serve as references for the fossils. Ten total human references were included, five male and five female. Before aligning the human femora with the fossil femora, femoral head measurements were taken for the human models in the same fashion as the fossil measurements. Once initial measurements were taken, the process of aligning the references with the fossils began. Each fossil femur was aligned with the ten reference femora. The basic procedure consisted of three steps. The first was to cut the reference in order to keep only the landmarks present in the fossil. For example, KNM-ER 1505 consisted of only a head and neck, so when it was aligned with the references, everything except for the head and neck was removed from the references using the segmentation tool. Additionally, if the fossil and reference were not ipsilateral, the x-axis of the reference was adjusted to form a mirror image that could be superimposed with the fossil. The second step was to roughly align them in the 3-D

space using the translation/rotation tool to line up important structures such as the fovea and trochanters. Once the two meshes were roughly aligned, the third step was to conduct fine registration to generate a statistical matrix and heat map that assessed the degree of shape and size variation between the point clouds, or meshes, that represented the structures of the bones. These steps are illustrated in Figure 3.

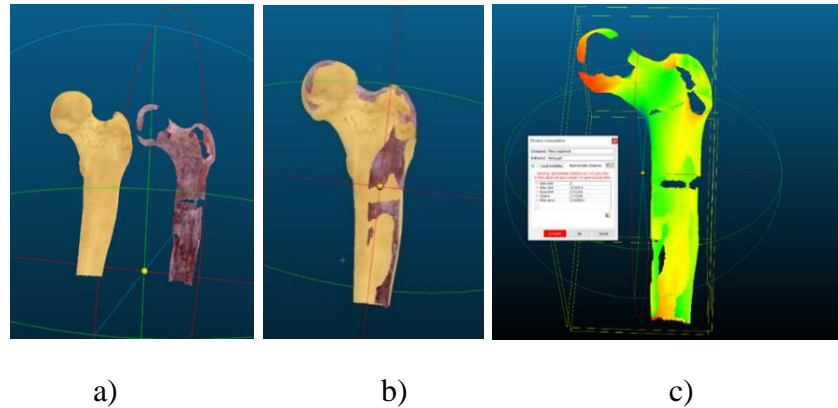


Figure 3: Alignment Process

Image “a” depicts a human reference being prepared for alignment with KNM-ER 1481. It has been segmented to match the anatomical landmarks present in the fossil femur and rotated to be in the same plane and position. In image “b” the reference has been roughly aligned with the fossil using the translate/rotate feature. Image “c” shows the final product of fine registration, which is a heat map with a statistical matrix that presents the degree of variation between the point clouds.

Another key component was the scaling factors used in the alignments. For the initial fine registrations with each pair, both the fossil and reference meshes were at a scale of 1. As mentioned in the background research, these fossils were expected to be slightly smaller than the human references given their suspected hominin species. With each alignment pair (five fossils paired with each of the ten references), the reference was scaled down until minimum sigma and standard deviation were observed. These were the most relevant metrics presented in the statistical matrix, so they were used to determine the most precise scaling factor for each

alignment pair. For each pair, the same alignment process was repeated an average of ten times or until the smallest possible values for sigma and standard deviation were identified. The scaling factors were tested within four decimal places (i.e., 0.9825 and 0.9850) to confirm accuracy of minimum values.

As the primary goal of aligning the fossils with human references was to obtain a metric that would allow for body mass estimation, the final step was to determine the femoral head diameter of the fossil based on the scaling factor of the reference. This was possible by multiplying the scaling factor by the head diameter of the reference femur. For example, if the best fit scaling factor was 0.75 and the reference's femoral head measured 40 mm, the fossil's head would be expected to measure approximately 30 mm. This enabled the comparison of the three methods for body mass reconstruction based on femoral head breadth. From this point, body masses were calculated, and statistical analyses were conducted for various stages of the procedure.

Results

Table 1 includes a description of each fossil, which regions of the femur are present, and whether the fossil's species is known or speculated in the literature. Table 2 shows the femoral head breadth of each fossil based on direct measurement with digital calipers (point picking). The values in Table 3 show the size of the femoral head estimated with the sphere-fitting technique. Table 4 includes femoral head breadth measurements for the reference femora.

Table 1: Fossil Specimen Descriptions

Specimen	Description	Species
KNM-ER 738	Proximal left femur with partial head, partial shaft	Possible <i>P. boisei</i>
KNM-ER 1472	Proximal right femur with partial head, partial shaft	Early <i>Homo</i> (<i>H. habilis</i> or <i>rudolfensis</i>)

KNM-ER 1481	Proximal left femur with partial head, partial shaft	Early <i>Homo</i> (<i>H. habilis</i> or <i>rudolfensis</i>)
KNM-ER 1503	Proximal left femur with partial head	Possible <i>P. boisei</i>
KNM-ER 1505	Nearly complete head and neck, side unidentified	Possible <i>P. boisei</i>

*Species predictions from Grabowski et al. 2015

Table 2: Fossil FHB Measurements

Fossil Specimen	FHB Range (mm)	FHB (mm)
KNM-ER 738	32.87-33.44	33.268
KNM-ER 1472	37.07-37.81	37.458
KNM-ER 1481	39.05-43.07	41.856
KNM-ER 1503	33.93-34.99	34.314
KNM-ER 1505	34.35-34.81	34.552

*FHB reported as a range and average of 5 separate measurements

Table 3: FHB by Sphere Approximation

Fossil Specimen	Range (mm)	Mean Radius (mm)	Mean Diameter (mm)
KNM-ER 738	16.75-17.1	16.95	33.9
KNM-ER 1472	17.9-19.1	18.44	36.88
KNM-ER 1481	20.5-21.2	21.0	42.0
KNM-ER 1503	16.8-17.5	17.04	34.08
KNM-ER 1505	16.8-17.3	17.18	34.36

*FHB reported as the range of 5 separate radius approximations, the mean of those approximations, and conversion to diameter.

Table 4: Reference FHB Measurements

Modern <i>H. sapiens</i> Reference	Sex	FHB (mm)
HOSAP 792R	M	44.91
HOSAP 496	M	45.72
HOSAP 928R	M	40.77
HOSAP 1158RR	M	42.99
HOSAP 1221	M	45.29
HOSAP 512	F	41.15
HOSAP 934	F	41.25
HOSAP 1027	F	37.17
HOSAP 1032	F	39.04

HOSAP 1109R	F	41.37
-------------	---	-------

*FHB reported as singular measurements. With complete models, there is less error in measuring the longest segment.

Table 5 demonstrates an example of the scaling process with KNM-ER 1472 and HOSAP 792R, and it reflects the statistical values presented in the alignment matrix. Notably, the minimum standard deviation was observed at scale factor of 0.9 while the minimum sigma was observed at scale factor of 0.83. Since Cloud Compare was a less familiar software, the difference between the two values was unknown in this context, as standard deviation and sigma tend to be interchangeable. Therefore, data was initially gathered for both values. Table 6 presents the most precise scaling factors for each alignment, with sigma values in the left column for each specimen and standard deviations in the right column. Figure 4 demonstrates the variation in the data from Table 6, with the x-axis following the same sequence as the rows, including the scaling factors for each alignment based on minimum values of sigma and standard deviation.

Table 5: Example Scaling Process and Statistical Values (KNM-ER 1472 with HOSAP 792R)

Scale Factor	Standard Deviation	Sigma	Mean Distance	Average Distance	Minimum Distance	Maximum Distance	Maximum Error
0.9025	2.160616	1.52757	1.497466	1.74213	0	9.03126	0.468249
0.9	2.114911	1.48517	1.39183	1.67002	0	8.41272	0.458952
0.8975	2.125155	1.46753	1.376762	1.65862	0	8.47199	0.470666
0.89	2.143686	1.45849	1.28085	1.63975	0	8.63685	0.457752
0.85	2.20997	1.38264	0.627241	1.47179	0	7.90721	0.519134
0.8325	2.19679	1.31866	0.308517	1.43493	0	7.2905	0.445338
0.83	2.201016	1.31537	0.25723	1.43588	0	7.44023	0.43842
0.8275	2.208087	1.31598	0.215749	1.43141	0	7.47452	0.44044
0.825	2.214731	1.33021	0.17452	1.42755	0	7.60562	0.522356
0.8225	2.22765	1.33542	0.136963	1.44487	0	7.35811	0.442906
0.8125	2.32154	1.4228	-0.022604	1.49516	0	7.52906	0.512288
0.8	2.319423	1.41553	-0.259448	1.50954	0	8.12056	0.507535

0.75	2.614342	1.77867	-1.172378	1.88215	0	9.39259	0.497806
0.7	2.898036	2.16692	-2.150924	2.49993	0	11.9603	0.496624

*Example scaled alignment with full statistical matrix included

Table 6: Scaling Factors

	738		1472		1481		1503		1505	
792R (M)	0.7725	0.7725	0.83	0.9	0.8785	0.879	0.8325	0.9375	0.75	0.75
496 (M)	0.685	0.6875	0.775	0.78	0.8225	0.85	0.78	0.87	0.7225	0.7225
512 (F)	0.8255	0.87	0.9055	0.9825	0.976	1.0125	0.9	1.0225	0.8025	0.8025
934 (F)	0.8575	0.8575	0.9225	0.9275	0.955	1.01	0.925	1.0075	0.7705	0.7705
928R (M)	0.875	0.875	0.945	0.945	0.9775	1	0.915	0.915	0.7925	0.7925
1588RR (M)	0.8525	0.8525	0.995	0.9975	1.0475	1.0475	0.935	1.02	0.7975	0.7975
1027 (F)	0.89	0.9375	0.9975	1.075	1.0375	1.0775	1.0125	1.1075	0.945	0.945
1032 (F)	0.839	0.839	0.94	0.94	0.96	0.96	0.945	0.995	0.8625	0.8625
1221 (M)	0.7975	0.8	0.8425	0.8725	0.9475	0.9475	0.855	1.0025	0.7775	0.78
1109R (F)	0.8375	0.9025	0.9375	1	0.9975	1.0725	0.9575	1.065	0.8625	0.9

*Minimum values of sigma (left) and standard deviation (right) for each alignment pair. Top headers refer to fossil specimens, while left side headers refer to human references.

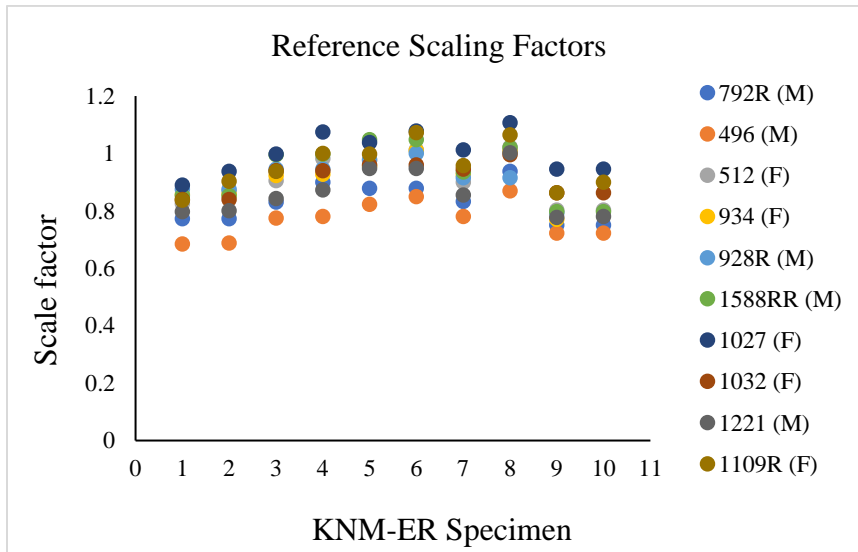


Figure 4: Scaling Factors

This graph illustrates the data from Table 6, showing the variation in scaling factors for each human reference. This became the foundation for rank correlation analysis.

Body masses were calculated using the most recently published least-squares and reduced major axis equations, based on the femoral head breadths that were determined through direct measurement, sphere-fitting and scaled alignment (Niskanen et al. 2018). The equations are as follows:

Least-squares (LS)

$$BM = 1.844(FHB) - 22$$

Reduced major axis (RMA)

$$BM = 3.163(FHB) - 85.224$$

Tables 7 and 8 reflect the calculated body masses for direct measurement, sphere approximation, and scaled alignment. Figures 6-7 depict these estimates and the variation associated with them. In Figures 5-7, the x-axis represents the five fossil femora, with 1=738, 2=1503, 3=1505, 4=1472, 5=1481.

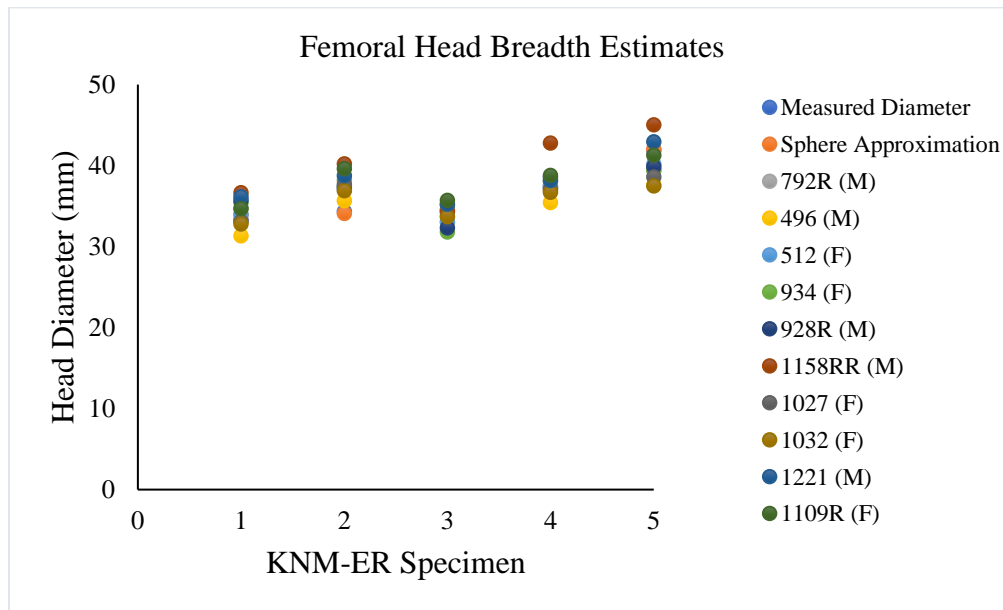


Figure 5: Femoral Head Diameters

This graph demonstrates the femoral head breadth of each fossil, determined through direct measurement, sphere approximation, and then based on the scaling factor for each reference. For the scale-based estimates, the best fit scaling factor was multiplied by the measured femoral head breadth of the associated human reference femur.

Table 7: Body Masses from LS Equation

	738 (kg)	1503 (kg)	1505 (kg)	1472 (kg)	1481 (kg)
Measured	39.346192	41.275016	41.713888	47.072552	55.182464
Sphere	40.51116	40.84352	41.35984	46.00672	55.448
792R (M)	41.97385	46.94269	40.11053	46.73565	50.75213
496 (M)	35.75076	43.75999	38.9123	43.33845	47.34307
512 (F)	40.63944	46.29254	38.89418	46.70988	52.05947
934 (F)	43.22574	48.36013	36.60808	48.16996	50.64208
928R (M)	43.7824	46.78959	37.58005	49.04499	51.48833
1158RR (M)	45.5807099	52.1207786	41.2206641	56.8771922	61.0390541
1027 (F)	39.001917	47.398249	42.771699	46.370126	49.111786
1032 (F)	38.39941	46.03032	40.09117	45.67037	47.11017
1221 (M)	44.60302	49.40512	42.93273	48.36119	57.13024
1109R (F)	41.88976	51.04411	43.79692	49.51839	54.09556

*Calculated using least-squares regression equation, $BM = 1.844(FHB) - 22$

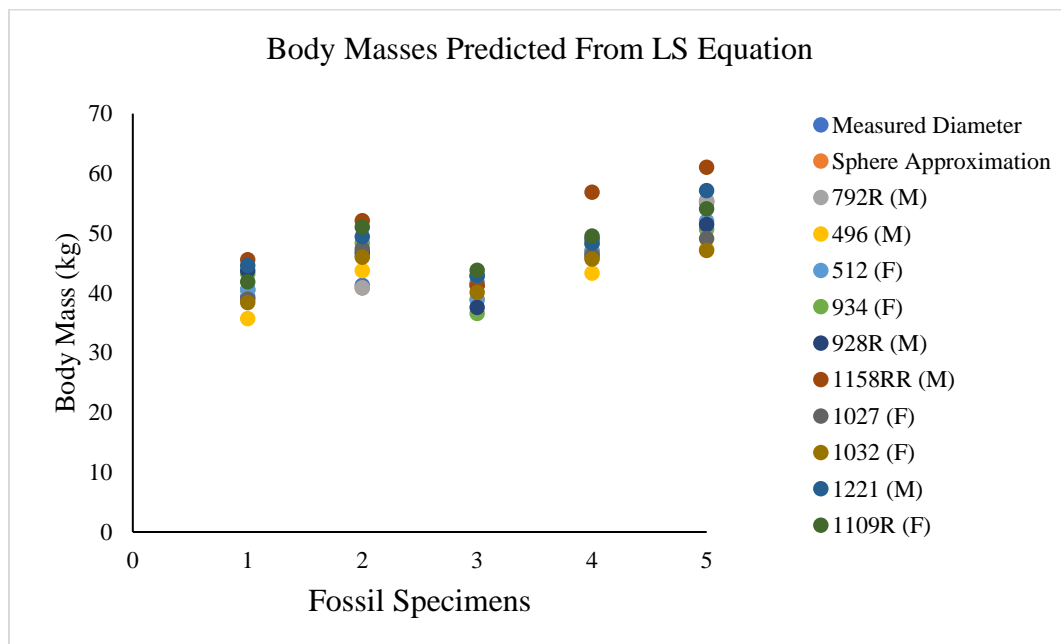


Figure 6: Body Masses Estimated from LS Equation

This graph illustrates the degree of variation in body mass estimates from Table 7.

Table 8: Body Masses Estimated from RMA Equation

	738 (kg)	1503 (kg)	1505 (kg)	1472 (kg)	1481 (kg)
Measured	20.002684	23.311182	24.063976	33.255654	47.166528
Sphere	22.0017	22.57104	23.45668	31.42744	47.622
792R (M)	24.50988	33.0329	21.31375	32.67777	39.56721
496 (M)	13.83547	27.57364	19.25843	26.85058	33.71967
512 (F)	22.22097	31.91771	19.22735	32.63357	41.80967
934 (F)	26.65724	35.46422	15.30602	35.13803	39.37843
928R (M)	27.61207	32.77029	16.97324	36.63896	40.83001
1158RR (M)	30.6967079	41.914841	23.2179526	50.0734832	57.2122951
1027 (F)	19.412152	33.814319	25.878431	32.050788	36.753537
1032 (F)	18.37867	31.46793	21.28054	30.85051	33.32018
1221 (M)	29.01969	37.25669	26.15464	35.46604	50.50753
1109R (F)	24.36565	40.06804	27.63698	37.45098	45.30218

*Calculated using reduced major axis equation, $BM = 3.163(FHB) - 85.224$

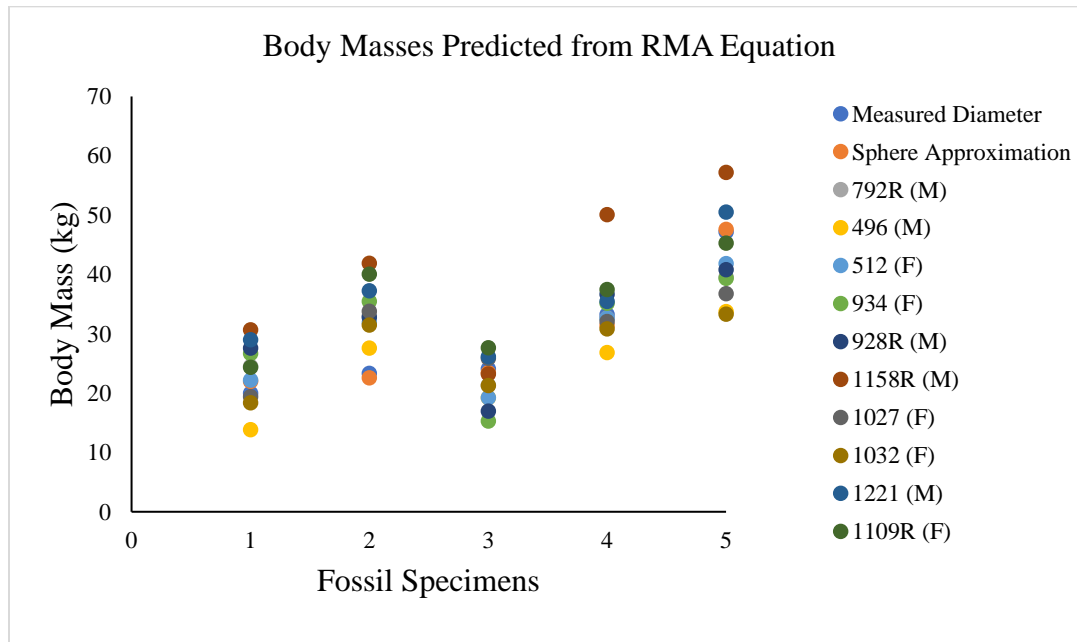


Figure 7: Body Masses Estimated from RMA Equation

This graph illustrates the degree of variation in body mass estimates from Table 8.

Analysis

To determine the precision of the scaling method, the scaling factors from Table 6 were ranked from the lowest to highest value, as shown in Table 9. A rank of 1 signifies the lowest scaling factor or the largest human reference, while a rank of 10 signifies the highest scaling factor or the smallest reference. Once the rankings were established, Spearman rank correlations were conducted. These correlations can only take place between two rank lists at a time, so the correlations between the rank orders of each fossil specimen were calculated, as demonstrated in Table 10. The purpose of this analysis was to establish the reliability of the scaled registrations. In an ideal scenario, the rankings for each reference would be the same for all fossil alignments, but morphological differences result in less precision, as indicated in Table 9 and Figure 8.

Table 9: Scale Rankings

	738	1472	1481	1503	1505
792R (M)	2	2	2	2	2
496 (M)	1	1	1	1	1
512 (F)	4	4	6	4	7
934 (F)	8	5	4	6	3
928R (M)	9	8	7	5	5
1588RR (M)	7	9	10	7	6
1027 (F)	10	10	9	10	10
1032 (F)	6	7	5	8	8
1221 (M)	3	3	3	3	4
1109R (F)	5	6	8	9	9

*Rankings are shown for the minimum sigma scaling factors, as those had slightly less variation than the scaling factors for minimum standard deviation. 792R, 496, 1027, and 1221 have the least variation in their rankings. In particular, 792R and 496 have the most optimal pattern of scaling, with no variation in their rank orders across the sample.

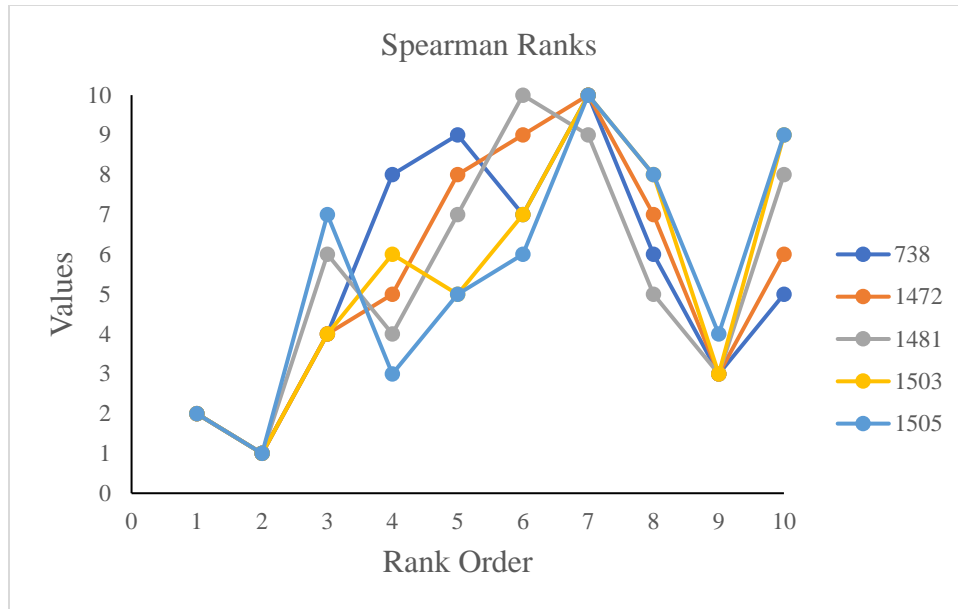


Figure 8: Spearman Ranks

This graph illustrates the variation in rank orders for the fossil specimens. The low and high end tended to be the most stable, with more variation in the middle.

Table 10: Spearman Rank Correlations

	738	1472	1481	1503	1505
738	1	0.90303	0.73333	0.75758	0.56364
1472	0.90303	1	0.90303	0.85455	0.74545
1481	0.73333	0.90303	1	0.80606	0.79394
1503	0.75758	0.85455	0.80606	1	0.87879
1505	0.56364	0.74545	0.79394	0.87879	1

*Rank lists of each fossil were correlated with the rank lists of all others in the sample. Range of correlation was 0.56364-0.90303, with only one pair below 0.7.

The other area of interest for analysis was body mass estimates. A major objective of this study was to determine whether scaled alignments produce equivalent results to the traditional methods. Variation of body mass estimates for each fossil was represented by calculating the standard deviation and coefficient of variation, as shown in Tables 11 and 12.

Table 11: Variation of LS Body Mass Estimates

	738	1503	1505	1472	1481
σ	2.847714108	3.462391359	2.210965	3.301449	4.1283
μ	41.22539857	46.68850443	40.49934	47.82296	52.61686
CV	0.069076691	0.074159398	0.054593	0.069035	0.07846

*All standard deviations greater than 2

Table 12: Variation of RMA Body Mass Estimates

	738	1503	1505	1472	1481
σ	4.884663625	5.939015112	3.792452	5.662952	7.081244
μ	23.22607358	32.59689994	21.98067	34.54282	42.76577
CV	0.210309487	0.182195703	0.172536	0.16394	0.165582

*All standard deviations greater than 2

While standard deviations were slightly higher than desired, this is likely due to the small sample size and the shape variation of the references. In reference to Tables 7 and 8, around half of the alignment-based estimates are within range of the measurement and sphere-based estimates. This supports what was also indicated in the Spearman ranks, which is that some references are reliable with scaled registrations, while others are more variable.

Discussion

The body mass estimates for this study were slightly more variable than expected, but that is likely a result of the fossil sample size and the shape variation of the reference models. Estimates from the RMA equation had more variation compared to estimates from the LS equation, which should be taken into account given that the RMA equation is considered to be a more effective predictor of body mass with scaling relationships (Ruff et al. 2018). However, others have made the opposite case, stating that RMA does not work as well for answering evolutionary questions (Hansen and Bartoszek 2012, Grabowski et al. 2015). The LS estimates

from this study were similar to prior estimates for the same fossils, which is encouraging. In Grabowski et al. 2015, *P. boisei* fossils were estimated to average 35-46 kg. The possible *P. boisei* in this sample, KNM-ER 738, 1503, and 1505, had average body masses of 41, 46, and 40 kg respectively. In the prior study, early *Homo* fossils were estimated to average 43-44 kg. The early *Homo* fossils included in this project, KNM-ER 1472 and 1481, had estimated average body masses of 47 and 52 kg respectively. The average body masses for this study include estimates from direct measurement, sphere approximation, and scaled alignments with all ten references. Because these estimates are within range of previous ones, it implies that the scaling method predicts mass reasonably accurately, at least some of the time. Despite the variation in this sample, the scaling approach resulted in satisfactory results. Approximately half of the scale-based estimates were within range of the estimates from direct measurement and sphere approximation, which indicates that the scaling approach has potential, but needs to be fine-tuned to be more reliable. In future studies that attempt to reconstruct body mass from scaled alignments, it would be beneficial to test the human references to ensure that they have a stable pattern of scaling. This could be accomplished by following the procedure from this project, selecting a larger group of references and determining which ones are most consistent via rank correlation.

This study had several limitations which should be considered in the interpretation of the results. The most obvious one is the small sample size, which contributed to significant statistical variation. In future studies, it would be advantageous to include more specimens in the sample to reduce variation and give the results more credibility. Additionally, the scaling method could be evaluated more accurately with references of known body mass. This would also account for the inherent error and biases in regression equations. Inverse calibration equations tend to

underestimate the projected range of values (Smith 1993, Uhl et al. 2013) and rarely have perfect correlations. For perspective, the equations used in this study had R-values of 0.583 (Niskanen et al. 2018). Aside from equation limitations, this study also had the potential for significant error based on the methods used. The alignments relied upon segmentation of the modern human references to fit the structures that were present, which was likely not as precise as it could have been, given the number of alignments necessary. After segmentation, there were still small parts of the references that had not been cut out and were not present in the fossils, and this contributed to slightly higher error in the fine registrations. However, this is only a minor concern given that the references were cut the same way every time, so the patterns shown by the scaling factors would not be likely to change if the references underwent more precise segmentation. There was also shape-related error in the alignments, as morphology and landmark scaling are expected to differ between fossil hominins and modern humans (Grabowski et al. 2015). A possible way to reduce both segmentation and shape-related error in future studies would be to isolate landmarks of the femur, such as the greater trochanter or the femoral head, and run scaled alignments on them. Outside of error and variation in the results, their generalizability is limited. This project only tested the alignment method on the femoral head, and while its principles suggest it could be applied to any anatomical structure, those have not yet been tested. However, the results from this study can inform future uses of scaled alignments in biological anthropology and even beyond the scope of this field.

Conclusion

Although there was significant variation in the sample body mass estimates and scaling factors, the scaling method shows potential as an alternative approach to reconstructing fossil hominin body masses. Further research to fine-tune its efficiency should include alignments with

isolated landmarks to reduce variation from shape differences. However, the findings from this study suggest that scaled alignments can serve as a valuable tool for estimating body masses from fossil fragments that are challenging to measure accurately using traditional methods.

References

1. Antón, Susan, Potts, Richard, and Leslie Aiello. 2014. "Evolution of Early *Homo*: An Integrated Biological Perspective." *Science* 345 (6192). doi:10.1126/science.1236828
2. Auerbach, Benjamin, and Christopher Ruff. 2004. "Human Body Mass Estimation: A Comparison of "Morphometric" and "Mechanical" Methods." *American Journal of Physical Anthropology* 125 (4): 331–342. doi:10.1002/ajpa.20032
3. Churchill, Stephen, and Caroline Vansickle. 2017. "Pelvic Morphology in *Homo erectus* and Early *Homo*." *The Anatomical Record* 300 (5): 964–977. doi:10.1002/ar.23576
4. Elliott, Marina, Kurki, Helen, Weston, Darlene, and Mark Collard. 2016. "Estimating Body Mass from Skeletal Material: New Predictive Equations and Methodological Insights from Analyses of a Known-Mass Sample of Humans." *Archaeological and Anthropological Sciences* 8 (4): 731–750. doi:10.1007/s12520-015-0252-5
5. Grabowski, Mark, Hatala, Kevin, Jungers, William, and Brian Richmond. 2015. "Body Mass Estimates of Hominin Fossils and the Evolution of Human Body Size." *Journal of Human Evolution* 85: 75-93. doi:10.1016/j.jhevol.2015.05.005
6. Grine, Frederick, Jungers, William, Tobias, Phillip, and Osbjorn Pearson. 1995. "Fossil *Homo* Femur from Berg Aukas, Northern Namibia." *American Journal of Physical Anthropology* 97 (2): 151–185. doi:10.1002/ajpa.1330970207
7. Hammond, Ashley, Plavcan, Joseph M, and Carol Ward. 2013. "Precision and Accuracy of Acetabular Size Measures in Fragmentary Hominin Pelves Obtained Using Sphere-Fitting Techniques." *American Journal of Physical Anthropology* 150 (4): 565–578. doi:10.1002/ajpa.22228

8. Hansen, Thomas, and Krzysztof Bartoszek. 2012. "Interpreting the Evolutionary Regression: The Interplay Between Observational and Biological Errors in Phylogenetic Comparative Studies." *Systematic Biology* 61 (3): 413-425. doi: 10.1093/sysbio/syr122
9. Holliday, Trenton, Hutchinson, Vance, Morrow, Melissa, and Glen Livesay. 2010. "Geometric Morphometric Analyses of Hominid Proximal Femora: Taxonomic and Phylogenetic Considerations." *Journal of Comparative Human Biology* 61 (1): 3-15. doi:10.1016/j.jchb.2010.01.001
10. Kappelman, John. 1996. "The Evolution of Body Mass and Relative Brain Size in Fossil Hominids." *Journal of Human Evolution* 30 (3): 243–276. doi:10.1006/jhev.1996.0021
11. Mahfouz, Mohamed, Merkl, Brandon, Fatah, Emam, Booth, Robert, and Jean-Noël Argenson. 2007. "Automatic Methods for Characterization of Sexual Dimorphism of Adult Femora: Distal Femur." *Computer Methods in Biomechanics and Biomedical Engineering* 10 (6): 447-456. doi: 10.1080/10255840701552093
12. McHenry, Henry. 1992. "Body Size and Proportions in Early Hominids." *American Journal of Physical Anthropology* 87 (4): 407-431. doi:10.1002/ajpa.1330870404
13. Niskanen, Markku, Junno, Juho-Antti, Maijanen, Heli, Holt, Brigitte, Sladěk, Vladimir, and Margit Berner. 2018. "Can We Refine Body Mass Estimations Based on Femoral Head Breadth?" *Journal of Human Evolution* 115:112-121. doi:10.1016/j.jhevol.2017.10.015
14. Plavcan, Joseph M. 2012. "Body Size, Size Variation, and Sexual Size Dimorphism in Early *Homo*." *Current Anthropology* 53 (S6): S409 - S423. doi:10.1086/667605
15. Plavcan, Joseph M, Meyer, Valentine, Hammond, Ashley, Couture, Christine, Madelaine, Stéphane, Holliday, Trenton, Maureille, Bruno, Ward, Carol, and Erik Trinkaus. 2014.

- “The Regourdou 1 Neandertal Body Size.” *Comptes Rendus Palevol* 13 (8): 747-754.
doi:10.1016/j.crpv.2014.07.003
16. Ruff, Christopher. 1991. “Climate and Body Shape in Hominid Evolution.” *Journal of Human Evolution* 21 (2): 81–105. doi:10.1016/0047-2484(91)90001-C
 17. Ruff, Christopher. 1994. “Morphological Adaptation to Climate in Modern and Fossil Hominids.” *American Journal of Physical Anthropology* 37 (S19): 65–107.
doi:10.1002/ajpa.1330370605
 18. Ruff, Christopher, Trinkaus, Erik, and Trenton Holliday. 1997. “Body Mass and Encephalization in Pleistocene *Homo*.” *Nature* 387 (6629): 173–176.
doi:10.1038/387173a0
 19. Ruff, Christopher, and Markku Niskanen. 2018. “Introduction to Special Issue: Body Mass Estimation- Methodological Issues and Fossil Applications.” *Journal of Human Evolution* 115: 1-7. doi:10.1016/j.jhevol.2017.09.011
 20. Smith, Richard. 1993. “Bias in Equations Used to Estimate Fossil Primate Body Mass.” *Journal of Human Evolution* 25 (1): 31-41. doi: 10.1006/JHEV.1993.1036
 21. Spocter, Muhammad, and Paul Manger. 2007. “The Use of Cranial Variables for the Estimation of Body Mass in Fossil Hominins. *American Journal of Physical Anthropology* 134 (1): 92–105. doi:10.1002/ajpa.20641
 22. Uhl, Natalie, Rainwater, Christopher, and Lyle Konigsberg. 2013. “Testing for Size and Allometric Differences in Fossil Hominin Body Mass Estimation.” *American Journal of Physical Anthropology* 151 (2): 215–229. doi:10.1002/ajpa.22269

23. Will, Manuel, Pablos, Adrian, and Jay Stock. 2017. "Long-Term Patterns of Body Mass and Stature Evolution Within the Hominin Lineage." *Royal Society Open Science* 4 (11). doi:10.1098/rsos.171339